International Journal of
Proteomics & Bioinformatics

Research Article

Effects of Mutations of Phosphorylation Sites in Sars-Cov-2 Encoded Nucleocapsid Protein on its Dimerization -

Pierre Limtung and H Y Lim Tung*

Peptide and Protein Chemistry Research Laboratory, Nacbraht Biomedical Research Institute, New York City, USA

***Address for Correspondence:** H Y Lim Tung, Peptide and Protein Chemistry Research Laboratory, Nacbraht Biomedical Research Institute, 3164 21st Street, Suite 122, Astoria (NYC), NY 11106, USA, Tel: 332-201-7161; E-mail: hyltung2010@nacbrahtbiomedresins.org

Submitted: 08 February 2021; **Approved:** 25 February 2021; **Published:** 27 February 2021

Cite this article: Limtung P, Lim Tung HY. Effects of Mutations of Phosphorylation Sites in Sars-Cov-2 Encoded Nucleocapsid Protein on its Dimerization. Int J Proteom Bioinform. 2021 Feb 27;6(1): 003-009.

ABSTRACT

Mutations in several phosphorylation sites within the phosphorylation rich domain of SARS-COV-2 Nucelocapsid protein (NCp), including phospho-serines 186, 197 and 202, and C-TAK1 phosphorylation recognition sites phospho-serine 197 within the motif RNpSTP, and arginine 203 and glycine 204 within the motif RGTpSP have been described and have been proposed to prevent the binding and sequestration of NCp by Protein 14-3-3. Here, through structure modeling and thermodynamic calculation, it is shown that mutations of serines 186, 197 and 202 to phenylalanine, leucine and asparagine, and arginine/glycine 203/204 to lysine/arginine or lysine/threonine resulted in significant stabilization of the NCp-NCp complex through increase in Stability Energy ($\Delta G_{stability\ energy}$) and Binding Energy ($\Delta\Delta G_{binding\ energy}$). These results suggest that SARS-COV-2 has evolved through the above described mutations in NCp to enhance NCp's dimerization and its activity as an essential co-factor for the replication, transcription and packaging of the SARS-COV-2 genome.

INTRODUCTION

SARS-COV-2 Nucleocapsid protein (NCp) plays an essential role as a co-factor in the initiation and control of the replication, transcription and packaging of the SARS-COV-2 genome [1-6]. Dimerization of SARS-COV-2 Nucleocapsid protein (NCp) is an important step in the replication, transcription and packaging of the SARS-COV-2 genome [7-12]. Oligomerization of NCp is also required for the packaging of SARS-COV-2 genome [8-12]. Phosphorylation of NCp within a phosphorylation rich domain has been proposed to play an important role in the control of NCp functions [3,13-18]. Recent work has described the existence of a cellular response mechanism for preventing dimerization of NCp involving phosphorylation dependent sequestration of monomeric NCp by Protein 14-3-3 [13,18]. The phosphorylation rich domain located in the linker region of NCp is exposed at its surface and contains two recognition and binding sites (RNpSTP and RGTpSP) for Protein 14-3-3 [13,18]. Other phosphorylations sites, including serines 186 and 202, and threonines 198 and 205 are also present in the phosphorylation rich domain of NCp [13,18].

Phosphorylation sites 186, 197 and 202 are mutated to phenylalanine, leucine and asparagine in SARS-COV-2 strains/sub-strains from Iran, Spain and India respectively [13]. Phosphorylation recognition sites within the RNpSTP and RGTpSP motifs that are recognized by C-TAK1 [13,18-21], including phospho-serine 197, arginine 203 and glycine 204 are mutated to leucine, lysine and arginine or lysine and threonine in SARS-COV-2 strains/sub-strains isolated from Israel, Italy, Poland, Bangladesh, Greece and Czech republic [13]. The significance of these mutations has not been clearly established. Here, we use structure model analysis, and thermodynamic calculation to study the effects of these mutations on the dimerization of NCp. The results provide evidence that mutations in the phosphorylation sites and phosphorylation recognition sites phospho-serines 186, 197 and 202, arginine 203 and glycine 204 increase the Stability Energy ($\Delta G_{stability\ energy}$) and Binding Energy ($\Delta\Delta G_{binding\ energy}$) of NCp-NCp compex. It is submitted that SARS-COV-2 has evolved to optimize the dimerization of NCp through mutations of at least 3 phosphorylation sites, phospho-serines 186, 197 and 202 and phosphorylation recognition sites, phospho-serine 197, arginine 203 and glycine 204.

METHODS

The de novo rendering of the structure of dephospho-NCp using the Quark Program pursuant to Xu and Zhang, et al. [22,23] was as described previously [13]. Phosphorylation of SARS-COV-2 Nucleocapsid protein (NCp) was performed with FoldX using the Build Model Program pursuant to Guerois et al. and Schymkowitz, et al. [24,25]. Mutation of amino acid residues within NCp was aperformed with FoldX using the Build Model program pursuant Guerois, et al. and Schymkowitz, et al. [24,25]. Docking experiments to identify the dimerization of NCp were performed using the ZDOCK program pursuant to Pierce, et al. [26]. NCps rendered in this work and Protein 14-3-3 (1YZ5) based on the structure determination of Benzinger, et al. [27] were analyzed and visualized by the CCP4 Molecular Graphics Program Version 2.10.11 as described by Mc Nicolas, et al [28] and the ZMM Molecular Modeling Program as described by Garden and Zhorov [29].

Determination and calculation of Stability Energy ($\Delta G_{stability\ energy}$) of the protein complexes was performed using the Stability Program of FoldX as described by Guerois, et al. and Schymkowitz, et al. [24,25]. Binding Energy ($\Delta\Delta G_{binding\ energy}$) of protein complex was determined and calculated using the Analyze Complex Program of FoldX as described by Guerois, et al. and Schymkowitz, et al. [24,25]. Binding Energy Difference ($\Delta\Delta\Delta G_{binding\ enrgy\ difference}$) between phospho-NCps complex and mutant phospho-NCps complex was calculated pursuant to Teng, et al. and Nishi, et al. [30-32] from the equation: $\Delta\Delta\Delta G_{binding\ energy\ difference} = \Delta\Delta G_{binding\ energy}$ (binding energy of phospho-NCp-14-3-3 complex) - $\Delta\Delta G_{binding\ energy}$ (binding energy of dephospho-NCp-14-3-3 complex.

RESULTS

The effects of mutations in the phosphorylation sites of NCp were determined with respect to the binding of dephospho-NCp, mutant dephospho-NCp, phospho-NCp and mutant phospho-NCp to themselves. Figure 1 and figure 2 represent docking experiments of dephospho-NCp and mutant S186F-NCp with themselves. Both dephospho-NCp and mutant S186F-NCp readily form complexes. Major difference in conformations of dephospho-NCp and mutant S186F-NCp could be observed. The Stability Energy ($\Delta G_{stability\ energy}$) and Binding Energy ($\Delta\Delta G_{binding\ energy}$) of dephospho- NCp dimer were calculated to be ~698 Kcal/mol and 91 Kcal/mol respectively while the calculated Stability Energy ($\Delta G_{stability\ energy}$) and Binding Energy ($\Delta\Delta G_{binding\ energy}$) of mutant S186F-NCp dimer was calculated to be ~770 Kcal/mol and ~168 respectively. These results suggest that mutation of serine 186 of NCp to phenylalanine 186 was accompanied by enhanced stabilization and binding affinity between the two components of the NCp dimer. The Binding Energy Difference ($\Delta\Delta\Delta G_{binding\ energy\ difference}$) between dephospho-NCp dimer and mutant S186F-NCp dimer was calculated to be ~78 Kcal/mol. Pursuant to Teng et al. and Nishi et al. [30-32], positive Binding Energy Difference ($\Delta\Delta\Delta G_{binding\ energy\ difference}$) is thermodynamic evidence of stabilization and increase of binding efficiency.

Table 1 depicts the thermodynamic calculations of Stability Energy ($\Delta G_{stability\ energy}$), Binding Energy ($\Delta\Delta G_{binding\ energy}$) and Binding Energy Difference ($\Delta\Delta\Delta G_{binding\ energy\ difference}$) of the dimerization of various NCp mutants with respect to dephospho-NCP dimer. The dimers of mutants S197L and S202N were associated with decreased Stability

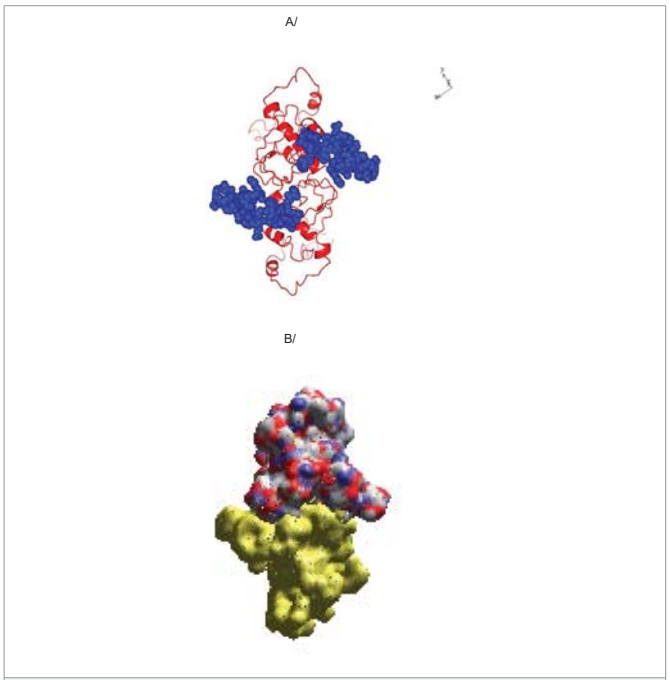

Figure 1: A: Ribbon structure (red) of dephospho-SARS-COV-2 Nucleocapsid protein (NCp) dimer, rendered as described in Method Section. Phosphorylation rich domain is shown as blue spheres. B: Realistic rendering of dephospho-SARS-COV-2 Nucleocapsid protein (NCp) complex (component 1 is colored red and blue while component 2 is colored yellow).

Table 1: Thermodynamic calculations, including Stability Energy (ΔG stability), Binding Energy (ΔΔG binding energy) and Binding Energy Difference (ΔΔΔG binding energy difference) that underlie the dimerization of dephospho-NCp and various mutant-NCps.

	Stability Energy (ΔG) Kcal/mol	Binding Energy (ΔΔG) Kcal/mol	Binding Energy Difference (ΔΔΔG) Kcal/mol
-Dephospho-NCp-NCp complex	**~698**	**~90**	**~ 000**
-S186F mutant-NCp-NCp complex	~770	~168	~ 078
-Phospho-serine 186-S197L mutant-NCp-NCp complex	~689	~87	~ -03
-Phospho-serine 186-S202N mutant-NCp-NCp complex	~675	~67	~ -23
-Phospho-serine 186-RG203/204KR mutant-NCp-NCp complex	~737	~136	~ 046
-Phospho-serine 186-RG203/204KT mutant-NCp-NCp complex	~759	~156	~ 066

Energy ($\Delta G_{stability\ energy}$) and Binding Energy ($\Delta\Delta G_{binding\ energy}$). However, the dimers of mutants RG203/204KR-NCp and RG203/204KT-NCp were associated with significant increase of Stability Energy ($\Delta G_{stability\ energy}$), Binding Energy and positive Binding Energy Difference ($\Delta\Delta\Delta G_{binding\ energy\ difference}$) in comparison to dephospho-NCp dimer. These results are indicative of enhanced binding affinity between the NCp mutants.

Figure 3 illustrates the docking of phospho-serine 186-NCp. There was considerable difference in the conformations of phospho-serine 186-NCp and mutant S186F-NCp dimers (compare figure 2 with figure 3). The calculated Stability Energy ($\Delta G_{stability\ energy}$) and Binding Energy ($\Delta\Delta G_{binding\ energy}$) of phospho-serine 186 NCp dimer were ~667 Kcal/mol and 63 Kcal/mol respectively while the calculated Stability Energy ($\Delta G_{stability\ energy}$) and Binding Energy ($\Delta\Delta G_{binding\ energy}$) of mutant S186F-NCp dimer was ~770 Kcal/mol and ~168 respectively. These results are evidence that mutation of phospho-serine 186 of NCp to phenylalanine 186 was accompanied by enhanced stabilization and binding affinity between the two components of the NCp dimer. The Binding Energy Difference ($\Delta\Delta\Delta G_{binding\ energy\ difference}$) between phospho-serine 186-NCp dimer and mutant S186F-NCp dimer was calculated to be ~105 Kcal/mol, confirming thermodynamic stabilization and enhancement of binding efficiency between the molecules of the NCp dimer.

Figures 4 and 5 show the dimerizations of phospho-serine 197-NCp and phospho-serine 197-S186F mutant-NCp. The results show that both phospho-serine 197-NCp and phospho-serine 197-S186F mutant-NCp form dimers and there was marked difference in their conformations. The calculated Stability Energy ($\Delta G_{stability\ energy}$) and Binding Energy ($\Delta\Delta G_{binding\ energy}$) of phospho-serine197-NCp dimer were ~699 Kcal/mol and ~87 Kcal/mol respectively whereas the Stability Energy ($\Delta G_{stability\ energy}$) and Binding Energy ($\Delta\Delta G_{binding\ energy}$) of the phospho-serine197-S186F mutant-NCp dimer were ~788 Kcal/mol and ~184 Kcal/mol respectively. The Binding Energy Difference ($\Delta\Delta\Delta G_{binding\ energy\ difference}$) between phospho-serine 197-NCp dimer and phospho-serine197-S186F mutant-NCp dimer was calculated to be ~97 Kcal/mol, evidencing enhanced thermodynamic stabilization and binding affinity between the components of the phospho-serine197-S186F mutant-NCp in the NCp dimer.

Figures 6 and 7 summarizes the docking experiments of phospho-serine 202-NCp and phospho-serine 202-S186F mutant-NCp with themselves. Both phospho-serine 202-NCp and phospho-serine 202-S197L mutant-NCp form dimers with recognizable difference

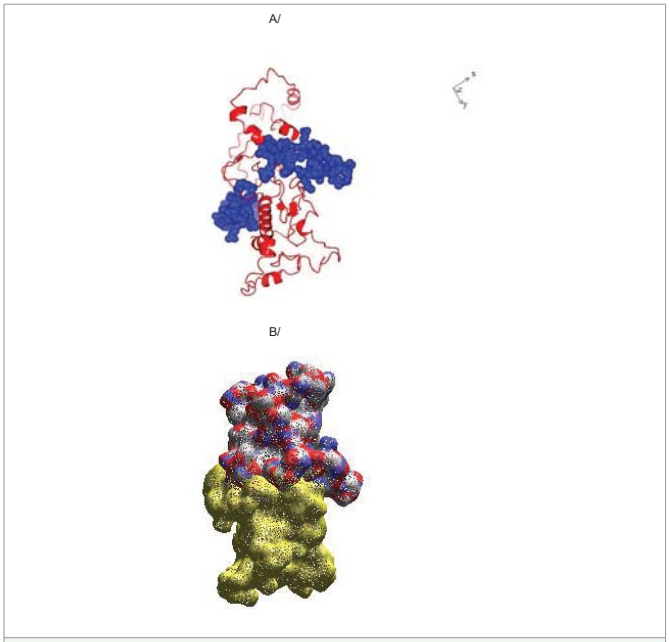

Figure 2: A: Ribbon structure (red) of S186F mutant-SARS-COV-2 Nucleocapsid protein (NCp) and Protein 14-3-3 complex, rendered as described in Method Section. Blue spheres show the phosphorylation rich domain, B: Realistic rendering of S186F mutant SARS-COV-2 Nucleocapsid protein (NCp) complex (component 1 is colored red and blue while component 2 is colored yellow).

in the conformation of their respective dimers. The Stability Energy ($\Delta G_{stability\ energy}$) and the Binding Energy ($\Delta\Delta G_{binding\ energy}$) of the phospho-serine 202-NCp dimer were calculated to be ~696 Kcal/mol and 95 Kcal/mol respectively. The Stability Energy ($\Delta G_{stability\ energy}$) and the Binding Energy ($\Delta\Delta G_{binding\ energy}$) of the phospho-serine 202-S186F mutant-NCp dimer were calculated to be 761 Kcal/mol and ~165 Kcal/mol respectively. The Binding Energy Difference ($\Delta\Delta\Delta G_{binding\ energy\ difference}$) between the dimers of phospho-serine 202-NCp and phospho-serine 202-S197L mutant-NCp was ~70 Kcal/mol. These results are consistent with the conclusion that mutation of serine 186 to phenylalanine caused enhanced stability and binding affinity of between the components in the NCp dimer.

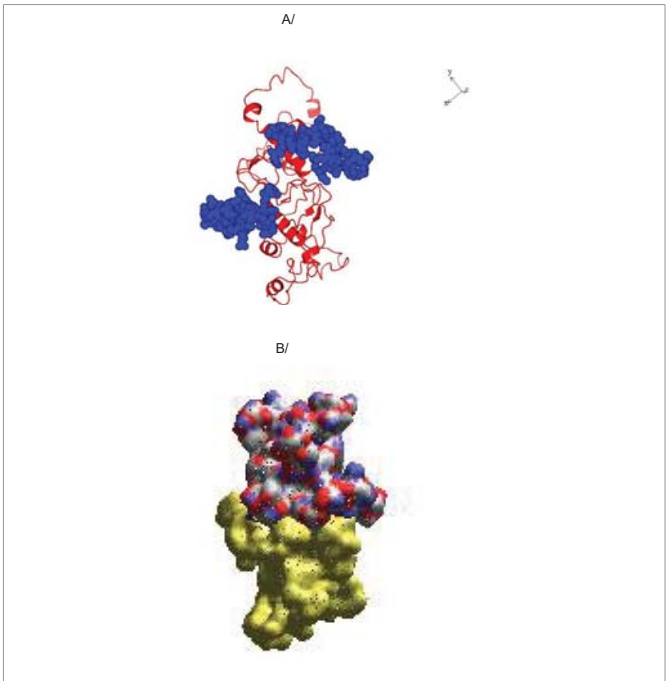

Figure 3: A: Ribbon structure (red) of phospho-serine 197-SARS-COV-2 Nucleocapsid protein (NCp) dimer. Blue spheres show the phosphorylation rich domain of NCp), rendered as described in Method Section. B: Realistic rendering of phospho-197-SARS-COV-2 Nucleocapsid protein (NCp) dimer (component 1 is colored red and blue while component 2 is colored yellow).

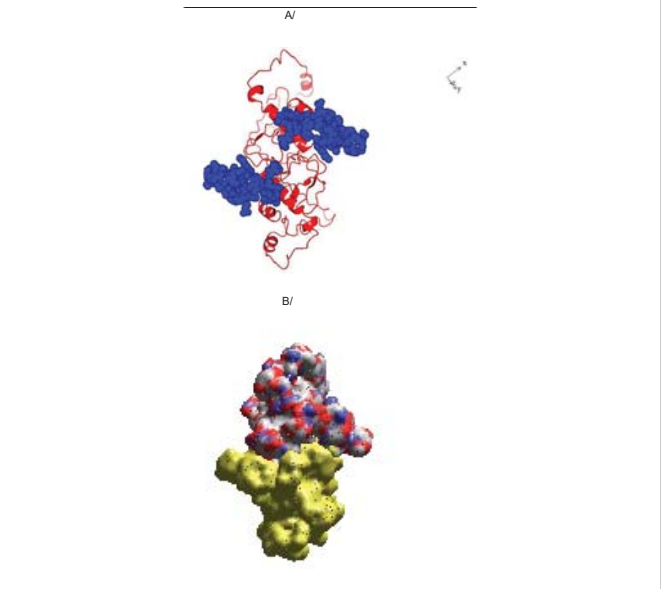

Figure 4: A: Ribbon structure (red) of phospho-serine 197-SARS-COV-2 Nucleocapsid protein (NCp) dimer. Blue spheres show the phosphorylation rich domain of NCp), rendered as described in Method Section. B: Realistic rendering of phospho-186-SARS-COV-2 Nucleocapsid protein (NCp) dimer. (Component 1 is colored red and blue while component 2 is colored yellow).

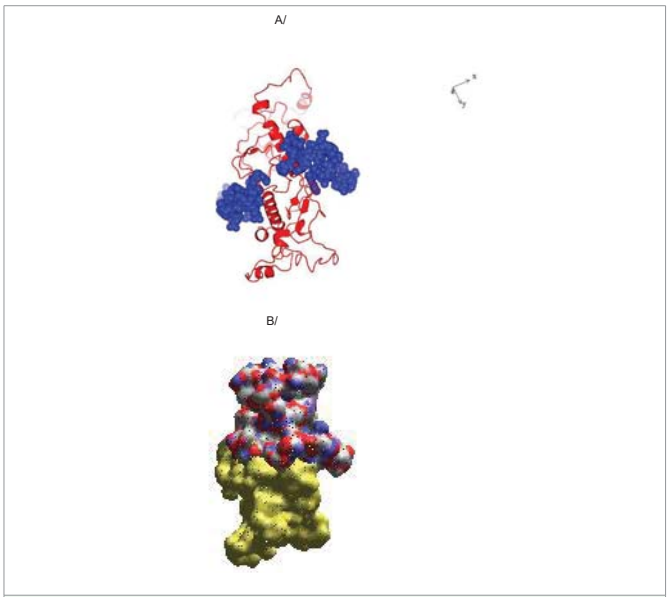

Figure 5: A: Ribbon structure (red) of phospho-serine 197-S186F mutant-SARS-COV-2 Nucleocapsid protein (NCp) dimer. Blue spheres show the phosphorylation rich domain of NCp), rendered as described in Method Section. B: Realistic rendering of phospho-186-SARS-COV-2 Nucleocapsid protein (NCp) dimer. (Component 1 is colored red and blue while component 2 is colored yellow).

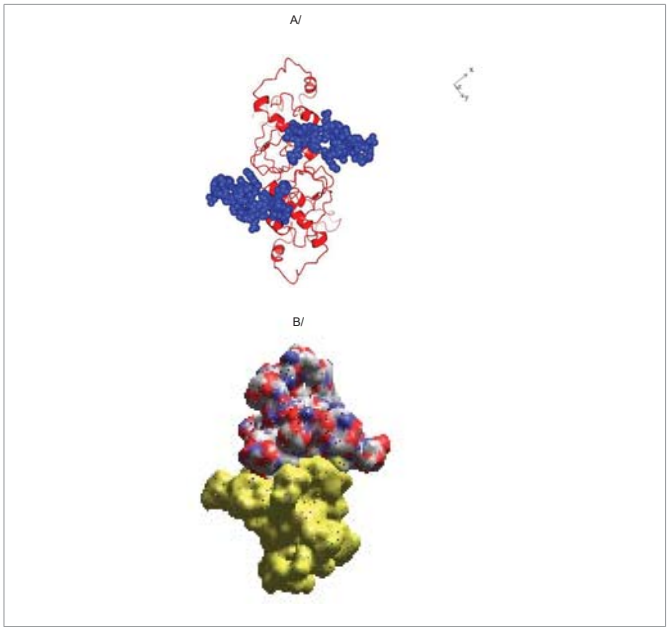

Figure 6: A: Ribbon structure (red) of phospho-serine 202-SARS-COV-2 Nucleocapsid protein (NCp) dimer. Blue spheres show the phosphorylation rich domain of NCp), rendered as described in Method Section. B: Realistic rendering of phospho-serine 202-SARS-COV-2 Nucleocapsid protein (NCp) dimer ((component 1 is colored red and blue while component 2 is colored yellow).

Table 2 summarizes the thermodynamic calculations of various

NCp mutant-Protein 14-3-3 complexes. The results showed that like mutations of serines 186, 197 and 202 of NCp, mutations of arginine 203 and glycine 204 within the motif RGTpSP to lysine 203 and arginine 204 or lysine 203 and threonine 204 were accompanied by significant increase in Stability Energy ($\Delta G_{stability\ energy}$) and Binding Energy ($\Delta\Delta G_{binding\ energy}$). Calculation of Binding Energy Difference ($\Delta\Delta\Delta G_{binding\ energy\ difference}$) between the various reference phospho-NCps and mutant-NCps confirms that the above mutations were indeed accompanied by significant increase in stability and binding efficiency of the respective NCps.

DISCUSSION

It was previously shown that phosphorylation of serines 186, 197 and 202 of NCp cause a decrease in Stability Energy and Binding Energy of NCp in its dimer [13,18]. Mutations in the phosphorylation sites, serine 186, 197 and 202, and phosphorylation recognition sites, phospho-serine 197, arginine 203 and glycine 204 within the motifs RNpSTP and RGTpSP to leucine, lysine 203 and arginine 204 or lysine 203 and threonine 204 respectively were identified in strains/sub-strains isolated from individuals located in various parts of the world [13]. It was proposed that mutations in the phosphorylation sites and phosphorylation recognition motifs allow NCp to evade sequestration by Protein 14-3-3 which would result in enhanced dimerization of NCp, an important essential step for NCp to act as a co-factor for the replication, transcription and packaging of the SARS-COV-2 genome [13,18]. The present work provides evidence that mutations in the phosphorylation sites, serines 186, 197 and 202, and phosphorylation recognition sites, phospho-serine 197, arginine 202 and glycine 203 within the motifs RNpSTP and RGTpSP were accompanied by significant enhancement of the stability and binding affinity of the NCp dimer.

While there is a phosphorylation dependent cellular response mechanism to bind, sequester and inhibit the functions of NCp by

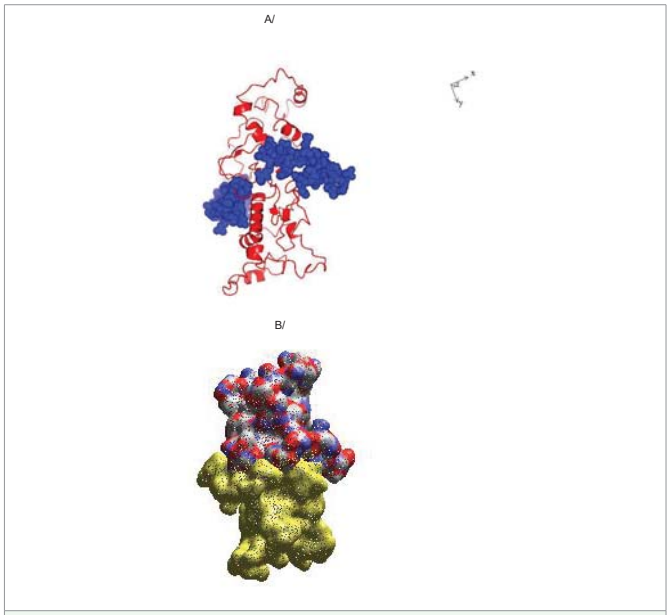

Figure 7: A: Ribbon structure (red) of phospho-serine 202-S186F mutant-SARS-COV-2 Nucleocapsid protein (NCp) dimer. Blue spheres show the phosphorylation rich domain of NCp), rendered as described in Method Section. B: Realistic rendering of phospho-202-S186F mutant-SARS-COV-2 Nucleocapsid protein (NCp) dimer (component 1 is colored red and blue while component 2 is colored yellow).

Table 2: Thermodynamic calculations, including Stability Energy (ΔG stability), Binding Energy (ΔΔG binding energy) and Binding Energy Difference (ΔΔΔG binding energy difference) that underlie the dimerization of various phospho-NCp and various mutant-NCps.

	Stability Energy (ΔG) Kcal/mol	Binding Energy (ΔΔG) Kcal/mol	Binding Energy Difference (ΔΔΔG) Kcal/mol
-Phospho-serine 186-NCp-NCp complex	**~667**	**~63**	**~ 000**
-S186F mutant-NCp-NCp complex	~770	~168	~ 105
-Phospho-serine 186-S197L mutant-NCp-NCp complex	~660	~62	~ -01
-Phospho-serine 186-S202N mutant-NCp-NCp complex	~658	~55	~ -08
-Phospho-serine 186-RG203/204KR mutant-NCp-NCp complex	~665	~67	~ 004
-Phospho-serine 186-RG203/204KT mutant-NCp-NCp complex	~668	~67	~ 004
-Phospho-serine 197-NCp-NCp complex	**~699**	**~87**	**~ 000**
-S197L mutant-NCp-NCp complex	~689	~87	~ 000
-Phospho-serine 197-S186F mutant-NCp-NCp complex	~788	~184	~ 097
-Phospho-serine 197-S202N mutant-NCp-NCp complex	~844	~239	~ 152
-Phospho-serine 197-RG203/204KR mutant-NCp-NCp complex	~734	~130	~ 043
-Phospho-serine 197-RG203/204KT mutant-NCp-NCp complex	~760	~157	~ 070
Phospho-serine 202-NCp-NCp complex	~696	~95	~ 000
-S202N-mutant-NCp-NCp complex	~689	~87	~ -08
-Phospho-serine 202-S186F mutant-NCp-NCp complex	~761	~165	~ 070
-Phospho-serine 202-S197L mutant-NCp-NCp complex	~737	~141	~ 046
-Phospho-serine 197-RG203/204KR mutant-NCp-NCp complex	~710	~111	~ 016
-Phospho-serine 197-RG203/204KT mutant-NCp-NCp complex	~756	~155	~ 060

Protein 14-3-3 in cells infected with SARS-COV-2, it is submitted that the latter has evolved to evade sequestration by Protein 14-3-3 through mutations of phosphorylation sites, S186F, S197L and S202N, and phosphorylation recognition sites, pS197L, RG203/204KR and RG203/204KT within the phosphorylation motifs, RNpSTP and RGTpSP [13,18]. It is also submitted that SARS-COV-2 has evolved through these mutations to enhance NCp's dimerization and its activity as an essential co-factor for the replication, transcription and packaging of the SARS-COV-2 genome (the present work).

Because of the essential role of NCp dimerization in the initiation and control of the replication, transcription and packaging of the SARS-COV-2 genome, drug discovery and vaccine development

programs that target NCp specifically are quite apparent [33-40]. However, from the above, it is clear that any drug discovery and vaccine development program that target NCp must take into account mutations in the phosphorylation sites (S186F, S197L and S202N) and phosphorylation recognition sites (phospho-serine 197, RG203/204KR and RG203/204KT) that occur within NCp in SARS-COV-2 strains and sub-strains that are seen in various populations and geographical areas. Molecules that act to enhance the sequestration of NCp by Protein 14-3-3 and prevent the dimerization of NCp are potential therapeutics for the control of SARS-COV-2 viability, infection and virulence. Molecules that act to prevent the dimerization of NCp at picomolar concentrations have been identified and are being characterized (Limtung, P. and Tung, H.Y.L., manuscript in preparation) [41,42].

ACKNOWLEDGEMENTS

This work was supported by the Nacbraht Biomedical Research Institute Fund.

REFERENCE

1. Stertz S, Reichel M, Spiegel M, Kuri T, Martínez-Sobrido L, García- Sastre A, Weber F, Kochs, G. The intracellular sites of early replication and budding of SARS coronavirus. Virology. 2007;36:304-315.
2. Verheije MH, Hagemeijer MC, Ulasli M, Reggiori, F, Rottier, PJ, Masters PS, de Haan CA. The coronavirus nucleocapsid protein is dynamically associated with the replication-transcription complexes. J Virol. 2010;84:11575-11579. https://tinyurl.com/a9cx9z3r
3. Cong Y, Ulasli M, Schepers H, Mauthe M, V'kovski P, Kriegenburg F, Thiel V, de Haan CAM, Reggiori F. Nucleocapsid Protein Recruitment to Replication-Transcription Complexes Plays a Crucial Role in Coronaviral Life Cycle. J Virol. 2020 Jan 31;94(4):e01925-19. doi: 10.1128/JVI.01925-19. PMID: 31776274; PMCID: PMC6997762.
4. Tylor S, Andonov A, Cutts T, Cao J, Grudesky E, Van Domselaar G, Li X, He R. The SR-rich motif in SARS-CoV nucleocapsid protein is important for virus replication. Can J Microbiol. 2009 Mar;55(3):254-60. doi: 10.1139/w08-139. PMID: 19370068.
5. Chen CY, Chang CK, Chang YW, Sue SC, Bai HI, Riang L, Hsiao CD, Huang TH. Structure of the SARS coronavirus nucleocapsid protein RNA-binding dimerization domain suggests a mechanism for helical packaging of viral RNA. J Mol Biol. 2007 May 11;368(4):1075-86. doi: 10.1016/j.jmb.2007.02.069. Epub 2007 Mar 2. PMID: 17379242; PMCID: PMC7094638.
6. Hsieh PK, Chang SC, Huang CC, Lee TT, Hsiao CW, Kou YH, Chen, IY, Chang CK, Huang TH, Chang MF. Assembly of severe acute respiratory syndrome coronavirus RNA packaging signal into virus-like particles is nucleocapsid dependent. J Virol. 2005;79:13848-13855.
7. Yu IM, Gustafson CLT, Diao J, Burgner II JW, Li Z, Chen J. Recombinant Severe Acute Respiratory Syndrome (SARS) Coronavirus Nucleocapsid Protein Forms a Dimer through Its C-terminal Domain. J Biol Chem. 2005;280:23280-23286.
8. He R, Dobie F, Ballantine M, Leeson A, Li Y, Bastien N, Cutts T, Andonov A, Cao J, Booth TF, Plummer FA, Tyler S, Baker L, Li X. Analysis of multimerization of the SARS coronavirus nucleocapsid protein. Biochem Biophys Res Commun. 2004 Apr 2;316(2):476-83. doi: 10.1016/j.bbrc.2004.02.074. PMID: 15020242; PMCID: PMC7111152.
9. Peng TY, Lee KR, Tarn WY. Phosphorylation of the arginine/serine dipeptide-rich motif of the severe acute respiratory syndrome coronavirus nucleocapsid protein modulates its multimerization, translation inhibitory activity and cellular localization. FEBS J. 2008 Aug;275(16):4152-63. doi: 10.1111/j.1742-4658.2008.06564.x. Epub 2008 Jul 9. PMID: 18631359; PMCID: PMC7164085.
10. Surjit M, Liu B, Kumar P, Chow VT, Lal SK. The nucleocapsid protein of the SARS coronavirus is capable of self-association through a C-terminal 209 amino acid interaction domain. Biochem Biophys Res Commun. 2004 May 14;317(4):1030-6. doi: 10.1016/j.bbrc.2004.03.154. PMID: 15094372; PMCID: PMC7111157.
11. Luo H, Ye F, Sun T, Yue L, Peng S, Chen J, Li G, Du Y, Xie Y, Yang Y, Shen J, Wang Y, Shen X, Jiang H. In vitro biochemical and thermodynamic characterization of nucleocapsid protein of SARS. Biophys Chem. 2004 Dec 1;112(1):15-25. doi: 10.1016/j.bpc.2004.06.008. PMID: 15501572; PMCID: PMC7116930.
12. Chang CK, Sue SC, Yu TH, Hsieh CM, Tsai CK, Chiang YC, Lee SJ, Hsiao HH, Wu WJ, Chang CF, Huang TH. The dimer interface of the SARS coronavirus nucleocapsid protein adapts a porcine respiratory and reproductive syndrome virus-like structure. FEBS Letters. 2005;579:5663-5668.
13. Tung HYL, Limtung P. Mutations in the phosphorylation sites of SARS-CoV-2 encoded nucleocapsid protein and structure model of sequestration by protein 14-3-3. Biochem Biophys Res Commun. 2020 Oct 29;532(1):134-138. doi: 10.1016/j.bbrc.2020.08.024. Epub 2020 Aug 15. PMID: 32829876; PMCID: PMC7428706.
14. Surjit M, Kumar R, Mishra RN, Reddy MK, Chow VT, Lal SK. The severe acute respiratory syndrome coronavirus nucleocapsid protein is phosphorylated and localizes in the cytoplasm by 14-3-3-mediated translocation. J Virol. 2005 Sep;79(17):11476-86. doi: 10.1128/JVI.79.17.11476-11486.2005. PMID: 16103198; PMCID: PMC1193639.
15. Wu CH, Yeh SH, Tsay YG, Shieh YH, Kao CL, Chen YS, Wang SH, Kuo TJ, Chen DS, Chen PJ. Glycogen synthase kinase-3 regulates the phosphorylation of severe acute respiratory syndrome coronavirus nucleocapsid protein and viral replication. J Biol Chem. 2009;284:5229-5239.
16. Wu CH, Chen PJ, Yeh SH. Nucleocapsid phosphorylation and RNA helicase DDX1 recruitment enables coronavirus transition from discontinuous to continuous transcription. Cell Host Microbe. 2014 Oct 8;16(4):462-72. doi: 10.1016/j.chom.2014.09.009. PMID: 25299332; PMCID: PMC7104987.
17. Carlson CR, Asfaha JB, Ghent CM, Howard CJ, Hartooni N, Morgan DO. Phosphorylation modulates liquid-liquid phase separation of the SARS-CoV-2 N protein. bioRxiv [Preprint]. 2020 Jun 29:2020.06.28.176248. doi: 10.1101/2020.06.28.176248. Update in: Mol Cell. 2020 Dec 17;80(6):1092-1103.e4. PMID: 32637943; PMCID: PMC7337373.
18. Tung HY, Limtung P. Structure Model Analysis Of Phosphorylation Dependent Binding And Sequestration Of SARS-COV-2 Encoded Nucleocapsid Protein By Protein. BioRxiv. 2020. doi: 10.1101/2020.09.16.29936214-3-3.
19. Ogg S, Gabrielli B, Piwnica-Worms H. Purification of a serine kinase that associates with and phosphorylates human Cdc25C on serine 216. J Biol Chem. 1994 Dec 2;269(48):30461-9. PMID: 7982962.
20. Muller J, Ritt DA, Copeland TD, Morrison DK. Functional analysis of C-TAK1 substrate binding and identification of PKP2 as a new C-TAK1 substrate. EMBO J. 2003;22:4431-4442. doi: 10.1093/emboj/cdg426
21. Muslin AJ, Tanner JW, Allen PM, Shaw AS. Interaction of 14-3-3 with signaling proteins is mediated by the recognition of phosphoserine. Cell. 1996 Mar 22;84(6):889-97. doi: 10.1016/s0092-8674(00)81067-3. PMID: 8601312.
22. Yaffe MB, Rittinger K, Volinia S, Caron PR, Aitken A, Leffers H, Gamblin SJ, Smerdon SJ, Cantley LC. The structural basis for 14-3-3:phosphopeptide binding specificity. Cell. 1997;91:961-971. doi: 10.1016/S1097-2765(00)00114-3.
23. Xu D, Zhang Y. Ab initio protein structure assembly using continuous structure fragments and optimized knowledge-based force field. Proteins. 2012 Jul;80(7):1715-35. doi: 10.1002/prot.24065. Epub 2012 Apr 13. PMID: 22411565; PMCID: PMC3370074.
24. Xu D, Zhang Y. Toward optimal fragment generations for ab initio protein structure assembly. Proteins. 2013 Feb;81(2):229-39. doi: 10.1002/prot.24179. Epub 2012 Oct 16. PMID: 22972754; PMCID: PMC3551984.
25. Guerois R, Nielsen JE, Serrano L. Predicting changes in the stability of proteins and protein complexes: a study of more than 1000 mutations. J Mol

Biol. 2002 Jul 5;320(2):369-87. doi: 10.1016/S0022-2836(02)00442-4. PMID: 12079393.

26. Schymkowitz J, Borg J, Stricher F, Nys R, Rousseau F, Serrano L. The FoldX web server: an online force field. Nucleic Acids Res. 2005 Jul 1;33(Web Server issue):W382-8. doi: 10.1093/nar/gki387. PMID: 15980494; PMCID: PMC1160148.

27. Pierce BG, Wiehe K, Hwang H, Kim BH, Vreven T, Weng Z. ZDOCK server: interactive docking prediction of protein-protein complexes and symmetric multimers. Bioinformatics. 2014 Jun 15;30(12):1771-3. doi: 10.1093/bioinformatics/btu097. Epub 2014 Feb 14. PMID: 24532726; PMCID: PMC4058926.

28. Benzinger A, Popowicz GM, Joy JK, Majumdar S, Holak TA, Hermeking H. The crystal structure of the non-liganded 14-3-3sigma protein: insights into determinants of isoform specific ligand binding and dimerization. Cell Res. 2005 Apr;15(4):219-27. doi: 10.1038/sj.cr.7290290. PMID: 15857576.

29. McNicholas S, Potterton E, Wilson KS, Noble ME. Presenting your structures: the CCP4mg molecular-graphics software. Acta Crystallogr D Biol Crystallogr. 2011 Apr;67(Pt 4):386-94. doi: 10.1107/S0907444911007281. Epub 2011 Mar 18. PMID: 21460457; PMCID: PMC3069754.

30. Garden DP, Zhorov BS. Docking flexible ligands in proteins with a solvent exposure- and distance-dependent dielectric function. J Comput Aided Mol Des. 2010 Feb;24(2):91-105. doi: 10.1007/s10822-009-9317-9. Epub 2010 Jan 30. PMID: 20119653.

31. Teng S, Srivastava AK, Schwartz CE, Alexov E, Wang L. Structural assessment of the effects of amino acid substitutions on protein stability and protein protein interaction. Int J Comput Biol Drug Des. 2010;3(4):334-49. doi: 10.1504/IJCBDD.2010.038396. Epub 2011 Feb 4. PMID: 21297231; PMCID: PMC3319068.

32. Nishi H, Tyagi M, Teng S, Shoemaker BA, Hashimoto K, Alexov E, Wuchty S, Panchenko AR. Cancer missense mutations alter binding properties of proteins and their interaction networks. PLoS One. 2013 Jun 14;8(6):e66273. doi: 10.1371/journal.pone.0066273. PMID: 23799087; PMCID: PMC3682950.

33. Nishi H, Hashimoto K, Panchenko AR. Phosphorylation in protein-protein binding: effect on stability and function. Structure. 2011 Dec 7;19(12):1807-15. doi: 10.1016/j.str.2011.09.021. PMID: 22153503; PMCID: PMC3240861.

34. Kang S, Yang M, Hong Z, Zhang L, Huang Z, Chen X, He S, Zhou Z, Zhou Z, Chen Q, Yan Y, Zhang XS, Shan H, Chen S. Crystal structure of SARS-CoV-2 nucleocapsid protein RNA binding domain reveals potential unique drug targeting sites. Acta Pharma. Sinica. 2020;10:1228-1238.

35. Mukherjee D, Upasan R. SARS-CoV-2 nucleocapsid assembly inhibitors: Repurposing antiviral and antimicrobial drugs targeting nucleocapsid-RNA interaction. chemRxiv. doi:10.26434/chemrxiv.12587336.v2.

36. Yadav R, Imran M, Dhamija P, Suchal K, Handu S. Virtual screening and dynamics of potential inhibitors targeting RNA binding domain of nucleocapsid phosphoprotein from SARS-CoV-2. J Biomol Struct Dyn. 2020 Jun 22:1-16. doi: 10.1080/07391102.2020.1778536. Epub ahead of print. PMID: 32568013; PMCID: PMC7332875.

37. Liu SJ, Leng CH, Lien SP, Chi HY, Huang CY, Lin CL, Lian WC, Chen CJ, Hsieh SL, Chong P. Immunological characterizations of the nucleocapsid protein based SARS vaccine candidates. Vaccine. 2006 Apr 12;24(16):3100-8. doi: 10.1016/j.vaccine.2006.01.058. Epub 2006 Feb 8. PMID: 16494977; PMCID: PMC7115648.

38. Lin Y, Shen X, Yang RF, et al. Identification of an epitope of SARS-coronavirus nucleocapsid protein. Cell Research. 2003 Jun;13(3):141-145. doi: 10.1038/sj.cr.7290158.

39. Peng H, Yang LT, Wang LY, Li J, Huang J, Lu ZQ, Koup RA, Bailer RT, Wu CY. Long-lived memory T lymphocyte responses against SARS coronavirus nucleocapsid protein in SARS-recovered patients. Virology. 2006 Aug 1;351(2):466-75. doi: 10.1016/j.virol.2006.03.036. Epub 2006 May 11. PMID: 16690096; PMCID: PMC7111820.

40. Kalita P, Padhi AK, Zhang KYJ, Tripathi T. Design of a peptide-based subunit vaccine against novel coronavirus SARS-CoV-2. Microb Pathog. 2020 Aug;145:104236. doi: 10.1016/j.micpath.2020.104236. Epub 2020 May 4. PMID: 32376359; PMCID: PMC7196559.

41. Dutta NK, Mazumdar K, Gordy JT. The Nucleocapsid Protein of SARS-CoV-2: a Target for Vaccine Development. J Virol. 2020 Jun 16;94(13):e00647-20. doi: 10.1128/JVI.00647-20. PMID: 32546606; PMCID: PMC7307180.

42. Wang R, Hozumi Y, Yin C, Wei GW. Decoding SARS-CoV-2 Transmission and Evolution and Ramifications for COVID-19 Diagnosis, Vaccine, and Medicine. J Chem Inf Model. 2020; 60(12):5853-5865. DOI: 10.1021/acs.jcim.0c00501